DESIGN REFINEMENTS AND PROTOTYPING OF LEAD SHIELDING FOR THE FCC-ee ARC DIPOLES

R. Cowan*, G. Banks, B. Humann, A. Lechner, L. Jorat, K. Guergar, A. Romero Francia, R. Seidenbinder, A. Perillo Marcone, M. Calviani, J. Roaldsoy, M. Simoes, S. Sgobba, M. Morrone, V. Giovinco, A. Piccini, M. Timmins, J. Bauche, F. Carra, J. M. Madsen
CERN, Geneva, Switzerland

Abstract

In the Future Circular Collider (FCC-ee) at CERN, lead shielding will be required on the collider arc dipoles around synchrotron radiation (SR) absorber locations to reduce radiation levels in the tunnel and protect sensitive components. The shielding assemblies will be mounted around the yokes, where scattered SR photons are expected to deposit 10-15 MW of power in total (across all absorber locations combined over the entire collider) at the $t\bar{t}$ operating point. Between the yokes and the shielding, a water-cooling system will be integrated to cool both the shielding and the magnet. Recent design studies have focused on refining the geometry and cooling layout to simplify manufacturing, control costs and maintain shielding performance. A shielding prototype is planned to inform design choices and further improvements. This contribution presents the design evolution, plans for a prototype, and cooling system optimisations.

INTRODUCTION

The FCC-ee is presently envisioned as the next large scale collider to be built by CERN, as part of the larger FCC project. This lepton machine would collide electrons and positrons at up to 182.5 GeV in a 91 km tunnel under Switzerland and France [1]. The powerful synchrotron radiation (SR), 50 MW per beam, will be absorbed by approximately 26000 Synchrotron Radiation Absorbers (SRAs) distributed around the arcs [2]. These localise SR losses in an actively cooled copper absorber block within the vacuum chamber. At the highest energies foreseen, these SRAs do not completely shield the tunnel and surrounding environment from scattered radiation, so further shielding will be performed by lead blocks positioned around the SRAs. The blocks will be sufficiently thick to absorb the remaining ~10 MW of radiated power and reduce the dose in the tunnel upper cable trays from >100 kGy to <10 kGy at $t\bar{t}$ [3]. The mass of lead is estimated to be around 800 kg per unit and around 13000 units (one unit per two SRAs) will be needed in the arcs alone, totalling over 10000 tonnes of lead.

LEAD SHIELDING REFINEMENT

The lead shielding has been refined from the previous work [4] to be comprised of large cuboidal blocks, with the intention of reducing production costs. The lead insert, visible in Fig. 1, has been improved to better fit around the vacuum chamber. The sides and insert are extended to reduce shine paths forward and backwards. Additional design improvements being considered for implementation include a cut out in the region with highest power deposition to improve cooling, further integration refinements around the vacuum chamber, and custom geometries to minimise lead use.

* r.cowan@cern.ch

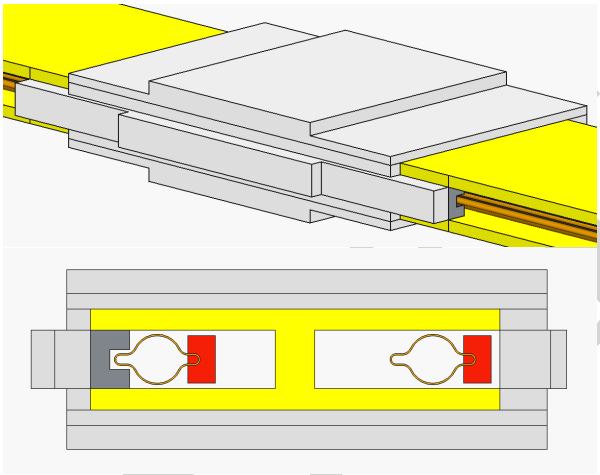

Figure 1: New design of lead shielding. Yoke - Yellow; Lead - Grey; Lead Insert - Dark grey; Vacuum chamber - Orange; SRAs (approx. position) - Red. The insert is the only piece of lead inside the aperture of the magnet yoke, and receives the highest energy deposition of all the lead, due to its proximity to the SRA.

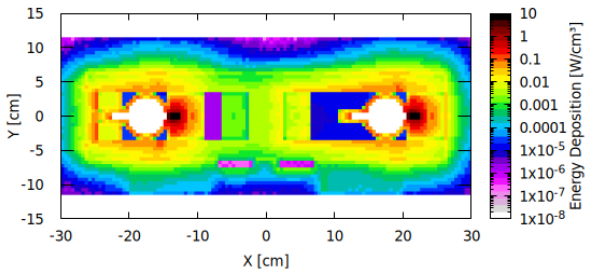

Figure 2: Power deposition in cross section of dipole and shielding, averaged over 1.3 m of shielding.

COOLING SYSTEM DESIGN

The lead, along with the steel yoke, together absorb a maximum of around 750 W per shielding unit [5] at $t\bar{t}$ for the LCC optics [6] (the yoke absorbs about 75% of this, for comparison, the two SRAs themselves absorb ~3.5 kW each). The distribution of the heating is shown in Fig. 2, generated using the FLUKA code [7–10].

This heat must be extracted from the lead through a dedicated cooling system, as if it were not directly cooled, the lead may melt with only poor natural air convection [4]. In addition, the tunnel air ventilation system would need to be excessively large and costly to handle the ~10 MW of heating over the ring. A limit of 250 kW was tentatively set on the convected power per arc sector (1/8th of the ring), and a limit of 87 °C was set on the maximum lead temperature, at a homologous temperature of 0.6, subject to further plastic deformation and creep studies. A number of options were considered for cooling, including clamping cooling pipes between lead blocks, casting lead around cooling pipes, and attaching cooling directly to the yoke, some of which have been discussed previously [4]. The current work explores the use of cooling plates as a method of removing heat from the system, and the effect on the convected power to the tunnel air.

Cooling Plates

Cooling plates are a widely used bespoke solution for removing large amounts of heat. They can be mass produced and provide excellent thermal contact compared to simple pipes due to their flat surfaces. They can also be used as structural components [11]. Current studies are considering aluminium plates for cost and thermal conductivity with stainless steel pipes for corrosion resistance. Two geometry options are studied here.

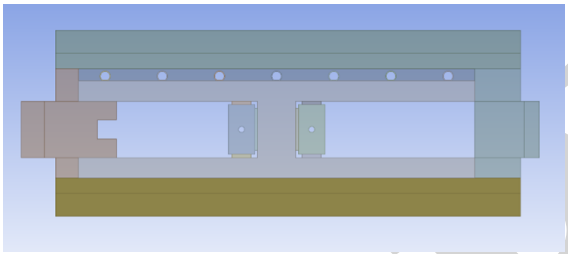

Figure 3: Top cooling option.

Top Cooling This option (Fig. 3) involves adding a large cooling plate on top of the yoke. This offers the largest surface area for cooling the yoke, but also provides a long thermal path to the bottom of the yoke and to the insert region, where the power deposition is high.

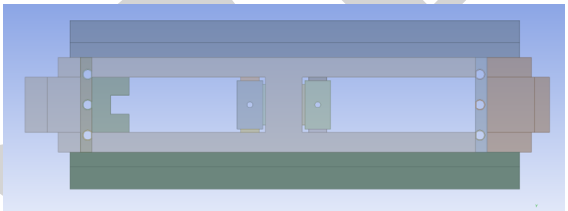

Figure 4: Side cooling option.

Side Cooling This option (Fig. 4) involves adding two smaller cooling plates to the sides of the yoke. The cooling contact area to the yoke is smaller, but evenly distributed between the top and bottom of the yoke. In addition, the inner cooling plate is very close to the insert, offering good cooling to this region.

Table 1: Operating Point Conditions

Condition	Value
Air temperature	32 °C
Air convection HTC	8 W/m^2 · K
Water temperature	27 °C
Water convection HTC	5000 W/m^2 · K
Water flow velocity	1 m/s

The two options were studied to evaluate their cooling performance. Using Ansys Workbench 2023b, the steady state temperatures in the yoke and lead were modelled, using initial assumptions given in Table 1. Common heat transfer correlations [12, 13] were used to estimate the heat transfer coefficients (HTCs) in water and air. Internal air convection was assumed at 1/4 of the external value. The energy deposition of the SR generated through FLUKA was used to apply heating to the lead and yoke. Due to unknown surface characteristics of lead and concern over the possible clamping force available between soft lead and cooling surfaces, low thermal contact conductivities (TCCs) were assumed between lead and other materials, and especially between lead and lead, as shown in Table 2. Later, these estimates will be improved in experimental tests. Initial sensitivity studies suggested the convected power is strongly dependant on the Steel (Yoke) to Cooling Plate connection, and the maximum lead temperature is dependant on the Lead to Cooling Plate connection and to a lesser extent on the Lead to Steel connection.

Table 2: Estimated thermal contact conductivities (TCCs) used for connections between differing materials.

Region 1	Region 2	TCC [W/m^2·K]
Steel	Cooling Plate	1000
Lead	Steel, Cooling Plate	200
Lead	Lead	10

Single Unit Results

The yoke and lead are sufficiently cooled by the plates in both the top and side cooling options at the initial operating point. The maximum lead temperature was 76.7 °C with top cooling (Fig. 5) and 71.2 °C with side cooling (Fig. 6), both well below the melting point of lead. However, the convected power to the air is lower for the top cooling, at 52 W vs 61 W for side cooling - 85 and 99 kW to an arc sector, respectively.

Series Units

Using the side cooling model, analysis was performed to estimate the effect of different environmental and cooling parameters over an extended set of cooling units. By modelling a single dipole unit at different water and air temperatures and linearising the relationship between these temperatures

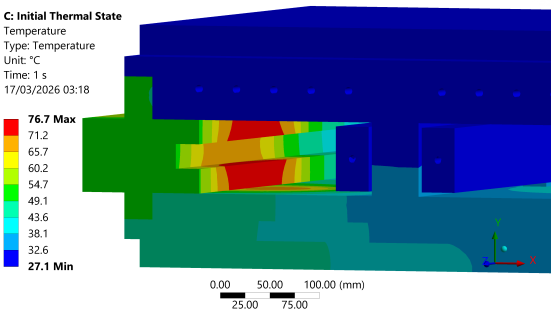

Figure 5: Top cooling - hotspot at 76.7 °C on insert region.

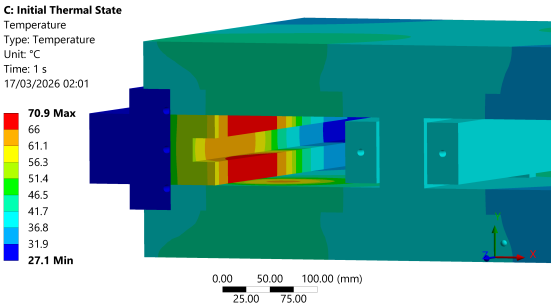

Figure 6: Side cooling - hotspot at 71.2 °C on insert region.

and the power transferred to each medium, the constants K_{AA} etc. in Eqs. (1) and (2) were calculated. For example, K_{AA} represents the variation in convected power when the temperature of air is increased by 1 degree.

$$P_{air} = K_{AA}T_{air} + K_{WA}T_{water} + c_A, \quad (1)$$

$$P_{water} = K_{AW}T_{air} + K_{WW}T_{water} + c_W. \quad (2)$$

Assuming that between each shielding unit the water flow is adiabatic, the water temperature rise over several shielding units connected in series can be calculated by iterating Eq. (3). We assume one shielding unit takes a flow of 8.4 l/min split between 2 flow loops at 1 m/s.

$$T_{N+1} = T_N + \frac{K_{AW}T_{air} + K_{WW}T_N + c_W}{C_p\dot{m}} \quad (3)$$

Series connection of shielding cooling plates reduces water usage, but also increases the temperature of the lead and convected power, as subsequent shielding units get sequentially hotter. It is assumed that shielding units are connected throughout at least one dipole (comprising 6 shielding units connected in series) to reduce connectors and water use to a manageable level. Connection of further dipoles in series and the effect on convected power to an arc sector is presented here; the same calculation process can be used for investigating the effect of the flow speed of water, of inlet water temperature, and of different heat transfer coefficients to the tunnel air.

Series Units Results

Figure 7 shows the strong variation in convected power with changes in air temperature. Only the single dipole option meets the 250 kW limit, and only when air temperature

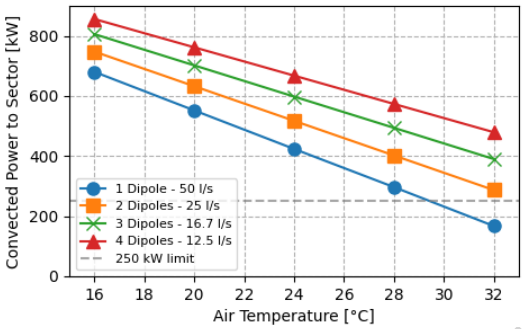

Figure 7: Effect of varying the number of dipoles connected in series on the convected power (Side cooling option).

is high. Currently this is considered acceptable, but studies are continuing to determine the best cooling configuration with respect to cost, air ventilation and lead temperatures.

PROTOTYPE OF SHIELDING UNIT

CERN is procuring a prototype to test the cooling performance of a single shielding unit, confirm TCCs in-situ, test the handling and structural behaviour of the lead during assembly, evaluate corrosion levels with aluminium cooling plates, and evaluate possible lead contamination risks. A preliminary design is shown in Fig. 8. It includes the yoke, lead and cooling plates, but not the vacuum chamber or SRAs, as these are considered thermally isolated enough to be excluded for this prototype.

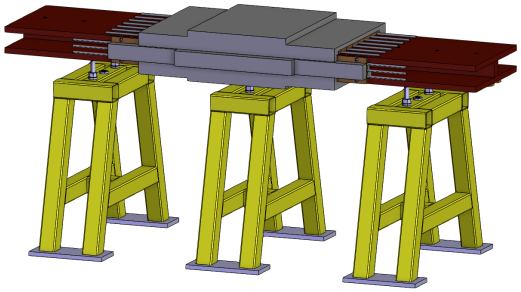

Figure 8: Prototype dipole with mounts and heaters.

The prototype will integrate both the side and top cooling options and compare their performance. Heating elements and control will be used to variously heat different components on the device, and cooling will be applied through the plates with a recirculating chiller. This will allow validation of the ANSYS model.

CONCLUSION

The lead shielding around the arc dipoles has been optimised for mass production and to improve shielding. The lead can be effectively cooled using a cooling plate solution, keeping its maximum temperature well below melting and reducing convected power. A prototype will be built in the summer of 2026 to permit refinements to modeling, cooling assessments, and to gain experience of lead handling.

REFERENCES

[1] M. Benedikt *et al.*, "Future circular collider feasibility study report – volume 2: accelerators, technical infrastructure and safety", *Eur. Phys. J. Spec. Top.*, vol. 234, pp. 5713–6197, 2025. doi:10.1140/epjs/s11734-025-01967-4

[2] M. Morrone, C. Garion, R. Kersevan, S. Rorison, and P. Chiggiato, "Preliminary design of the FCC-ee vacuum chamber absorbers", *J. Phys.: Conf. Ser.*, vol. 2687, p. 022011, Jan. 2024. doi:10.1088/1742-6596/2687/2/022011

[3] A. Lechner *et al.*, "FCC-ee radiation environment and shielding", in *Proc. IPAC'25*, Taipei, Taiwan, Jun. 2025, pp. 482–485. doi:10.18429/JACoW-IPAC2025-MOPM068

[4] A. R. Francia *et al.*, "Mechanical design and challenges of the FCCee arc radiation shielding", in *Proc. IPAC'25*, Taipei, Taiwan, Jun. 2025, pp. 2638–2641. doi:10.18429/JACoW-IPAC2025-THPB060

[5] B. Humann *et al.*, "Radiation environment in the FCC-ee arcs caused by synchrotron photon emission", presented at IPAC'26, Deauville, France, May 2026, paper MOP1014, this conference.

[6] P. Raimondi, S. M. Liuzzo, L. Farvacque, S. White, and M. Hofer, "Local chromatic correction optics for Future Circular Collider e+ e–", *Phys. Rev. Accel. Beams*, vol. 28, p. 021002, Feb. 2025. doi:10.1103/PhysRevAccelBeams.28.021002

[7] CERN, FLUKA Website. https://fluka.cern

[8] C. Ahdida *et al.*, "New capabilities of the FLUKA multi-purpose code", *Front. Phys.*, vol. 9, p. 788253, 2021. doi:10.3389/fphy.2021.788253

[9] G. Battistoni et al., "Overview of the FLUKA code", *Ann. Nucl. Energy*, vol. 82, pp. 10–18, 2015. doi:10.1016/j.anucene.2014.11.007

[10] G. Hugo *et al.*, "Latest FLUKA developments", *EPJ Nuclear Sci. Technol.*, vol. 10, p. 20, 2024. doi:10.1051/epjn/2024023

[11] C. Lacombe, Cold plate, Compelma, Jan. 2023, https://www.compelma.com/en/cold-plates/

[12] S. W. Churchill and H. H. S. Chu, "Correlating equations for laminar and turbulent free convection from a vertical plate", *Int. J. Heat Mass Transf.*, vol. 18, no. 11, pp. 1323–1329, Nov. 1975. doi:10.1016/0017-9310(75)90243-4

[13] F. W. Dittus and L. M. K. Boelter, "Heat transfer in automobile radiators of the tubular type", *Univ. Calif. Publ. Eng.*, vol. 2, pp. 433–461, 1930.